Atmos. Meas. Tech., 7, 2421–2435, 2014
www.atmos-meas-tech.net/7/2421/2014/
doi:10.5194/amt-7-2421-2014

Atmospheric Measurement Techniques
Open Access

Calibrated high-precision ^{17}O-excess measurements using cavity ring-down spectroscopy with laser-current-tuned cavity resonance

E. J. Steig[1,2], V. Gkinis[2,3], A. J. Schauer[1], S. W. Schoenemann[1], K. Samek[1], J. Hoffnagle[4], K. J. Dennis[4], and S. M. Tan[4]

[1]Δ*IsoLab, Earth & Space Sciences, and Quaternary Research Center, University of Washington, Seattle, WA 98195, USA
[2]Centre for Ice and Climate, Niels Bohr Institute, University of Copenhagen, 2100 Copenhagen, Denmark
[3]Institute of Arctic and Alpine Research, University of Colorado, Boulder, CO 80309, USA
[4]Picarro Inc. Santa Clara, CA 95054, USA

Correspondence to: E. J. Steig (steig@uw.edu)

Received: 7 October 2013 – Published in Atmos. Meas. Tech. Discuss.: 29 November 2013
Revised: 27 June 2014 – Accepted: 30 June 2014 – Published: 8 August 2014

Abstract. High-precision analysis of the $^{17}O/^{16}O$ isotope ratio in water and water vapor is of interest in hydrological, paleoclimate, and atmospheric science applications. Of specific interest is the parameter ^{17}O excess ($\Delta^{17}O$), a measure of the deviation from a linear relationship between $^{17}O/^{16}O$ and $^{18}O/^{16}O$ ratios. Conventional analyses of $\Delta^{17}O$ of water are obtained by fluorination of H_2O to O_2 that is analyzed by dual-inlet isotope ratio mass spectrometry (IRMS). We describe a new laser spectroscopy instrument for high-precision $\Delta^{17}O$ measurements. The new instrument uses cavity ring-down spectroscopy (CRDS) with laser-current-tuned cavity resonance to achieve reduced measurement drift compared with previous-generation instruments. Liquid water and water-vapor samples can be analyzed with a better than 8 per meg precision for $\Delta^{17}O$ using integration times of less than 30 min. Calibration with respect to accepted water standards demonstrates that both the precision and the accuracy of $\Delta^{17}O$ are competitive with conventional IRMS methods. The new instrument also achieves simultaneous analysis of $\delta^{18}O$, $\delta^{17}O$ and δD with precision of < 0.03 ‰, < 0.02 and < 0.2 ‰, respectively, based on repeated calibrated measurements.

1 Introduction

Measurements of the stable isotope ratios of water are ubiquitous in studies of earth's hydrological cycle and in paleoclimatic applications (Dansgaard, 1964; Dansgaard et al., 1982; Johnsen et al., 1995; Jouzel et al., 2007). Isotopic abundances are reported as deviations of a sample's isotopic ratio relative to that of a reference water, and expressed in the δ notation as

$$\delta^i = \frac{{}^iR_{\text{sample}}}{{}^iR_{\text{reference}}} - 1, \quad (1)$$

where ${}^2R = n(^2H)/n(^1H)$, ${}^{18}R = n(^{18}O)/n(^{16}O)$, ${}^{17}R = n(^{17}O)/n(^{16}O)$, and n refers to isotope abundance.

One important innovation was the development by Merlivat and Jouzel (1979) of a theoretical understanding of "deuterium excess":

$$d = \delta D - 8(\delta^{18}O), \quad (2)$$

where δD is equivalent to δ^2H. The deuterium excess is commonly used as a measure of kinetic fractionation processes. For example, deuterium excess variations from ice cores have been used to infer variations in evaporative conditions over the ocean surface areas from which polar precipitation is derived (Johnsen et al., 1989; Petit et al., 1991; Vimeux et al., 2001; Masson-Delmotte et al., 2005).

The $\delta^{18}O$ and δD isotopic values can be experimentally determined via a number of isotope ratio mass spectrometry (IRMS) techniques. For $\delta^{18}O$, equilibration with CO_2 has been the standard method for many decades (Cohn and Urey, 1938; McKinney et al., 1950; Epstein, 1953). For δD, reduction of water to H_2 over hot U (Bigeleisen et al., 1952; Vaughn et al., 1998) or Cr (Gehre et al., 1996) has typically

been used. Simultaneous determination of δ^{18}O and δD was made possible via the development of continuous-flow mass-spectrometric techniques utilizing conversion of water to CO and H_2 in a pyrolysis furnace (Begley and Scrimgeour, 1997; Gehre et al., 2004).

A recent innovation is the measurement of the difference between δ^{18}O and δ^{17}O at sufficiently high precision to determine very small deviations from equilibrium. In general, the nuclei mass differences of $+1n^0$ and $+2n^0$ (n^0 denotes a neutron) imply that the fractionation factor for δ^{17}O between two different phases will be approximately the square root of the fractionation factor for δ^{18}O (Urey, 1947; Craig, 1957; Mook, 2000):

$$\frac{^{17}R_\mathrm{a}}{^{17}R_\mathrm{b}} = \left(\frac{^{18}R_\mathrm{a}}{^{18}R_\mathrm{b}}\right)^{\lambda}, \tag{3}$$

where $\lambda = 0.5010$–0.5305 (Kaiser, 2008) and the subscripts "a" and "b" refer to different phases or samples. For isotopic equilibrium, the value of λ will approach θ, given theoretically by the ratio of the partition functions (Q), which in the limit of high temperature approaches a constant value given as follows (Matsuhisa et al., 1978):

$$\theta = \frac{\ln(Q_{17}/Q_{16})}{\ln(Q_{18}/Q_{16})} = \frac{\frac{1}{m_{16}} - \frac{1}{m_{17}}}{\frac{1}{m_{16}} - \frac{1}{m_{18}}} = 0.5305\,, \tag{4}$$

where m_{16} is the atomic mass of ^{16}O, m_{17} is that of ^{17}O, etc.[1]

By analyzing a set of meteoric waters, Meijer and Li (1998) estimated the value of λ to be 0.528. Barkan and Luz (2005) used careful water equilibrium experiments to determine an equilibrium value for λ of 0.529, while Barkan and Luz (2007) showed that λ is 0.518 under purely diffusive conditions, in good agreement with theory (Young et al., 2002). Thus, the Meijer and Li (1998) value of 0.528 for meteoric waters reflects the combination of equilibrium and diffusive processes in the hydrological cycle.

Based on these observations, Barkan and Luz (2007) defined the ^{17}O excess parameter as the deviation from the meteoric water line with slope of 0.528 in $\ln(\delta + 1)$ space:

$$\Delta^{17}\mathrm{O} = \ln(\delta^{17}\mathrm{O} + 1) - 0.528\ln(\delta^{18}\mathrm{O} + 1). \tag{5}$$

Like deuterium excess, ^{17}O excess is sensitive to kinetic fractionation but, unlike deuterium excess, it is nearly insensitive to temperature and much less sensitive than δD and δ^{18}O to equilibrium fractionation during transport and precipitation. Natural variations of Δ^{17}O in precipitation are orders of magnitude smaller than variations in δ^{18}O and δD and are typically expressed in per meg (10^{-6}) rather than per mil (10^{-3}).

[1]Note that the precise atomic masses should be used. $m_{16} = 15.99491462230 \pm 0.00000000016$, $m_{17} = 16.9991317 \pm 0.0000012$, and $m_{18} = 17.9991610 \pm 0.0000070$ (Audi et al., 2003).

The potential of Δ^{17}O in hydrological research is significant because it provides independent information that may be used to disentangle the competing effects of fractionation during evaporation, in transport, and in the formation and deposition of precipitation (Landais et al., 2008; Risi et al., 2010; Schoenemann et al., 2014). It also has applications in atmospheric dynamics because of the importance of supersaturation conditions that, during the formation of cloud ice crystals, impart a distinctive isotope signature to water vapor (e.g., Blossey et al., 2010; Schoenemann et al., 2014).

Compared to the routine nature of δ^{18}O and δD analysis, isotopic ratio measurements of ^{17}O, the second heavy isotope of oxygen in terms of natural abundance, are challenging. The greater abundance of ^{13}C than ^{17}O makes the measurement of δ^{17}O in CO_2 equilibrated with water by IRMS at $m/z = 45$ impractical. As a result, the precise measurement of Δ^{17}O requires conversion of water to O_2 rather than equilibration with CO_2 or reduction to CO. Meijer and Li (1998) developed an electrolysis method using $CuSO_4$. More recently, Baker et al. (2002) used a fluorination method to convert water to O_2, which was analyzed by continuous-flow IRMS; this approach was updated by Barkan and Luz (2005) for dual-inlet IRMS.

The dual-inlet IRMS method can provide high-precision and high-accuracy Δ^{17}O measurements. However, the technique is time consuming, resulting in significantly lower sample throughput when compared to the standard and relatively routine analysis of δ^{18}O and δD. The fluorination procedure requires 30 min or more per sample, while the dual-inlet mass-spectrometric analysis requires 2–3 h. In practice, multiple samples must be processed because of memory effects in the cobalt-fluoride reagent and other issues that can arise in the vacuum line (e.g., fractionation during gas transfer) (Barkan and Luz, 2005). Moreover, while this method provides the most precise available measurements of Δ^{17}O, measurements of individual δ^{18}O values by this method are generally less precise than those obtained with other approaches.

In recent years, laser absorption spectroscopy in the near-infrared and mid-infrared regions has increasingly been used for isotope analysis. An overview of experimental schemes for different molecules and isotopologues can be found in Kerstel (2004). In the case of water, laser absorption spectroscopy constitutes an excellent alternative to mass spectrometry. The main advantage is the ability to perform essentially simultaneous measurements of the water isotopologues directly on a water-vapor sample. As a result, tedious sample preparation and conversion techniques are not necessary. Commercialization of laser absorption spectrometers has recently allowed measurements of water isotope ratios to be performed with high precision and competitive relative accuracy, provided that a valid calibration scheme is applied (Brand et al., 2009; Gupta et al., 2009; Gkinis et al., 2010, 2011; Schmidt et al., 2010; Aemisegger et al., 2012; Kurita et al., 2012; Wassenaar et al., 2012).

The measurement of $^{17}O/^{16}O$ ratios should in principle not pose any additional challenges when compared to the measurement of $^{18}O/^{16}O$ and D/H. Provided that the absorption lines of interest are accessible by the laser source with no additional interferences from other molecules, a triple isotope-ratio measurement can be performed, resulting in calibrated values for $\delta^{18}O$, $\delta^{17}O$ and δD. In fact, triple isotope-ratio measurements of water have been presented in the past via the use of various laser sources utilizing different optical and data analysis techniques (Kerstel et al., 1999, 2002, 2006; Van Trigt et al., 2002; Gianfrani et al., 2003; Wu et al., 2010). However, with the exception of results presented recently by Steig et al. (2013) and Berman et al. (2013), precision has not been sufficient to be useful for applications requiring the detection of the very small natural variations in $\Delta^{17}O$.

In this work we report on development of a new cavity ring-down laser absorption spectrometer that provides both high-precision and high-relative-accuracy measurements of $\Delta^{17}O$. The instrument we discuss here is a modification, first described by Hsiao et al. (2012) and Steig et al. (2013), of the Picarro Inc. water isotope analyzer model L2130-*i*. It is now commercially available as model L2140-*i*. Critical innovations we introduced include the use of two lasers that measure absorption in two different infrared (IR) wavelength regions, and modifications to the spectroscopic measurement technique. We also developed a sample introduction system that permits the continuous introduction of a stable stream of water vapor from a small liquid water sample into the optical cavity. In combination with precise control of the temperature and pressure in the optical cavity of the instrument, data averaging over long integration times results in precision of better than 8 per meg in $\Delta^{17}O$. We establish the relative accuracy of our results in comparison with IRMS measurements. This work can also be seen as a demonstration of state-of-the-art performance for laser absorption spectroscopy isotope ratio analysis for all four main isotopologues of water ($H_2{}^{16}O$, $H_2{}^{17}O$, $H_2{}^{18}O$ and HDO).

2 Methods

2.1 Reporting of water isotope ratios

Normalization to known standards is critical in the measurement of water isotope ratios. By convention, $\delta^{18}O$ of a sample is relative to $^{18}O/^{16}O$ of VSMOW (Vienna Standard Mean Ocean Water) and normalized to $\delta^{18}O$ of SLAP (Standard Light Antarctic Precipitation). "Measured" δ values with respect to VSMOW are determined from the difference of "raw" values calculated directly from the ratio of measured isotopologue abundances:

$$\delta^{18}O_{\text{sample}}^{\text{measured}} = \frac{\delta^{18}O_{\text{sample}}^{\text{raw}} - \delta^{18}O_{\text{VSMOW}}^{\text{raw}}}{\delta^{18}O_{\text{VSMOW}}^{\text{raw}} + 1}, \quad (6)$$

where the subscript refers to an arbitrary sample. Normalization to SLAP is by

$$\delta^{18}O_{\text{sample}}^{\text{normalized}} = \delta^{18}O_{\text{sample}}^{\text{measured}} \frac{\delta^{18}O_{\text{SLAP}}^{\text{assigned}}}{\delta^{18}O_{\text{SLAP}}^{\text{measured}}}, \quad (7)$$

where $\delta^{18}O_{\text{SLAP}}^{\text{assigned}} = -55.5‰$ is the value assigned by the International Atomic Energy Agency (Gonfiantini, 1978; Coplen, 1988). δD is normalized in the same manner, using $\delta D_{\text{SLAP}}^{\text{assigned}} = -428‰$.

We normalize $\delta^{17}O$ using

$$\delta^{17}O_{\text{sample}}^{\text{normalized}} = \delta^{17}O_{\text{sample}}^{\text{measured}} \frac{\delta^{17}O_{\text{SLAP}}^{\text{assigned}}}{\delta^{17}O_{\text{SLAP}}^{\text{measured}}}. \quad (8)$$

There is no IAEA (International Atomic Energy Agency)-defined value for $\delta^{17}O_{\text{SLAP}}^{\text{assigned}}$, but Schoenemann et al. (2013) recommended that it be defined such that SLAP $\Delta^{17}O$ is precisely zero. We follow that recommendation here; that is, we define

$$\delta^{17}O_{\text{SLAP}}^{\text{assigned}} = e^{(0.528\ln(-55.5\times10^{-3}+1))} - 1\,, \quad (9)$$

which yields $\delta^{17}O_{\text{SLAP}}^{\text{assigned}} = -29.6986‰$, well within the error of published measurements (Barkan and Luz, 2005; Kusakabe and Matsuhisa, 2008; Lin et al., 2010; Schoenemann et al., 2013) after normalization to the associated $\delta^{18}O$ values (Schoenemann et al., 2013).

Throughout this paper, reported values of $\delta^{18}O$, $\delta^{17}O$, δD and $\Delta^{17}O$ have been normalized as described above unless specifically noted otherwise. Superscripts and subscripts are omitted except where needed for clarity.

2.2 $\Delta^{17}O$ analysis with mass spectrometry

IRMS measurements provide the benchmark for comparison with results from analysis of $\Delta^{17}O$ by CRDS (cavity ring-down spectroscopy). We used IRMS to establish accurate measurements of $\Delta^{17}O$ of five laboratory working standards and the IAEA reference water GISP (Greenland Ice Sheet Precipitation), relative to VSMOW and SLAP. We also used both IRMS and CRDS measurements to determine the δD and $\delta^{18}O$ of the same standards; $\delta^{17}O$ is calculated from the $\Delta^{17}O$ and $\delta^{18}O$ data. Table 1 reports the values, updated from those in Schoenemann et al. (2013).

We used the method described in Schoenemann et al. (2013) to convert water to O_2 by fluorination, following procedures originally developed by Baker et al. (2002) and Barkan and Luz (2005). A total of 2 µL of water are injected into a nickel column containing CoF_3 heated to 370 °C, converting H_2O to O_2, with HF and CoF_2 as byproducts. The O_2 sample is collected in a stainless steel cold finger containing 5A molecular sieve following Abe (2008). To minimize memory effects, a minimum of three injections are made prior to collecting a final sample for measurement.

Table 1. VSMOW-SLAP-normalized isotopic ratios of reference waters analyzed at the University of Washington "Δ*IsoLab". $\Delta^{17}O$ values are from long-term average IRMS measurements, updated from Schoenemann et al. (2013) to reflect the inclusion of additional data. $\delta^{18}O$ and δD values are from long-term average laser spectroscopy measurements. $\delta^{17}O$ values are calculated from $\Delta^{17}O$ and $\delta^{18}O$ (Eq. 5). Precision (±) is the standard error ($\sigma/\sqrt{n}$). n is the sample size.

	$\Delta^{17}O$ (per meg)	$\delta^{18}O$ (‰)	$\delta^{17}O$[a] (‰)	δD (‰)	n
GISP[b]	28 ± 2	-24.80 ± 0.02	-13.1444	-189.67 ± 0.20	20
VW	3 ± 3	-56.61 ± 0.02	-30.2980	-438.79 ± 0.35	10
WW	27 ± 2	-33.82 ± 0.03	-17.9754	-268.30 ± 0.31	36
SW	33 ± 2	-10.55 ± 0.02	-5.5515	-75.63 ± 0.17	18
PW	30 ± 2	-6.88 ± 0.02	-3.6087	-42.12 ± 0.18	17
KD[c]	-0.8 ± 4	0.43 ± 0.01	0.2262	1.33 ± 0.13	5

[a] $\delta^{17}O$ calculated from $\delta^{18}O$ and $\Delta^{17}O$. See Schoenemann et al. (2013). [b] CIAAW values for GISP are $\delta D = -189.73$ ‰ and $\delta^{18}O = -24.78$ ‰ (Gonfiantini et al., 1995). [c] Provisional measurement. Long-term average data for KD (Kona Deep) are not yet available.

The O_2 sample is analyzed on a ThermoFinnigan MAT 253 dual-inlet mass spectrometer at $m/z = 32$, 33, and 34 for $\delta^{18}O$ and $\delta^{17}O$, using O_2 gas as a reference. Each mass-spectrometric measurement comprises 90 sample-to-reference comparisons. Precise adjustment of both sample and reference gas signals (10 V±100 mV) permits long-term averaging with no measurable drift, so that the analytical precision is given by simple counting statistics: $\sigma/\sqrt{90}$, where σ is the standard deviation of the individual sample/reference comparisons. The resulting precision of repeated measurements of O_2 gas is 0.002, 0.004, and 0.0037 ‰ (3.7 per meg) for $\delta^{17}O$, $\delta^{18}O$, and $\Delta^{17}O$, respectively. Reproducibility of the $\delta^{17}O$ and $\delta^{18}O$ ratios of water samples is in practice less precise than these numbers indicate, because fractionation can occur during the fluorination process or during the collection of O_2. However, because this fractionation closely follows the relationship $\ln(\delta^{17}O + 1) = 0.528 \ln(\delta^{18}O + 1)$, the errors largely cancel in the calculation of $\Delta^{17}O$ (Barkan and Luz, 2005; Schoenemann et al., 2013). The reproducibility of the calibrated $\Delta^{17}O$ of repeated water samples ranges from 4 to 8 per meg (Schoenemann et al., 2013).

2.3 $\Delta^{17}O$ analysis with cavity ring-down spectroscopy

2.3.1 Instrument design

We used modified versions of a CRDS analyzer designed for $\delta^{18}O$ and δD, commercially available as model L2130-*i*, manufactured by Picarro Inc. The L2130-*i* is an update to the water-isotope analyzers originally discussed in Crosson (2008). It uses an Invar (Ni–Fe) optical cavity coupled to a near-infrared laser. Optical resonance is achieved by piezoelectric modifications to the length of the cavity. When the intensity in the cavity reaches a predetermined value, the laser source is turned off and the intensity then decays exponentially. The time constant of this decay is the "ring-down time". The ring-down time depends on the reflectivity of the mirrors, the length of the cavity, the mixing ratio of the gas being measured, and the frequency-dependent absorption coefficient. The frequency is determined with a wavelength monitor constructed on the principle of a solid etalon (Crosson et al., 2006; Tan, 2008).

Determination of $\delta^{18}O$ and δD ratios on the model L2130-*i* is obtained by measurements of the amplitude of $H_2{}^{18}O$, $H_2{}^{16}O$ and HDO spectral lines from a laser operating in the area of 7200 cm^{-1} (wavelength 1389 nm). In a modified version, which we refer to as the L2130-*i*-C, we added a second laser that provides access to another wavelength region, centered on 7193 cm^{-1}, where there are strong $H_2{}^{17}O$ and $H_2{}^{18}O$ absorption lines (Fig. 1). Rapid switching between the two lasers allows the measurement of all three isotope ratios essentially simultaneously. About 200–400 ring-down measurements are made per second, and complete spectra covering all four isotopologues are acquired in 0.8 s intervals.

For isotope measurements with the L2130-*i* or L2130-*i*-C under normal operating conditions, water vapor in a dry air or N_2 carrier gas flows continuously through the cavity to maintain a cavity pressure of (66.7 ± 0.1) hPa at a temperature of (80 ± 0.01) °C, normally at a H_2O mixing ratio of 20 mmol mol^{-1}. The flow rate of 40 $cm^3 min^{-1}$ (290 K, 10^5 Pa) is maintained by two proportional valves in a feedback loop configuration up- and down-stream of the optical cavity. The spectral peak amplitudes are determined from the least-squares fit of discrete measurements of the absorption (calculated from measurements of the ring-down time) to a model of the continuous absorption spectrum.

The spectroscopic technique utilized for the acquisition and analysis of the spectral region relevant to the measurement of the isotopologues of interest is essentially the same as the one used in the earlier commercially available L2130-*i* analyzer. One of the main features of this technique is that optical resonance is obtained by dithering the length of the cavity. As discussed in Results (Sect. 3), we found that drift on timescales longer than a few minutes limited the achievable precision of $\Delta^{17}O$ measurements to about 20 per meg;

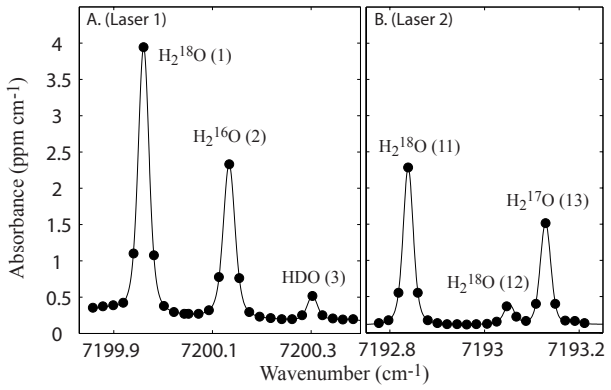

Figure 1. Measured absorption spectrum for water isotopologues in the two wavenumber regions used by the L2130-*i*-C and L2140-*i* CRDS analyzers. Filled circles: measured absorption for H_2O vapor 20 mmol mol^{-1} in dry air carrier, 66.7 hPa cavity pressure. The isotopologue associated with each peak is noted, with nominal peak numbers for reference (1–3 on laser 1, 11–13 on laser 2). Lines: least-squares fit to the data using Galatry profiles as discussed in the text.

this drift is ascribed to small but detectable drift in the wavelength monitor.

To improve measurement precision, we developed an updated version of the L2130-*i*-C, hereafter referred to as model L2140-*i*, which incorporates a different spectroscopic method. As in the L2130-*i*, a piezoelectric actuator is used to physically move one mirror of the cavity, and the wavelength monitor is used for feedback to the laser-frequency control electronics, thus allowing for rapid tuning to a target frequency. In the new method, though, the length of the optical cavity is kept constant during the acquisition of a spectrum, and resonance is obtained by dithering of the laser frequency by means of laser-current modulation. The frequency for each ring-down measurement is then determined directly from the resonance itself, based on the principle that resonance will occur only at frequencies spaced by integer multiples of the free spectral range (FSR) of the cavity (e.g., Morville et al., 2005).

The target frequency for each spectral region (e.g., that for $H_2{}^{17}O$) is determined in advance from measurements made at higher frequency resolution and used to tightly constrain the parameters in a spectral model (see below). The fine frequency spacing for a given narrow spectral region is determined only by the FSR. In this way, each ring-down measurement can be unambiguously assigned to a stable and equidistant frequency axis and the spectral line shape fit to a well-defined model; only a few data points are needed to precisely define each spectral peak. This new scheme also yields higher cavity excitation rates – typically 500 ring-downs per second.

The FSR is inversely proportional to the cavity length. The FSR of the L2130-*i* and L2140-*i* under normal operating conditions is 0.02 cm^{-1}, and varies by no more than 10^{-5} cm^{-1} owing to the precisely controlled temperature and pressure conditions. The cavity finesse is 44 000. The ring-down time constant for an empty cavity is 22 µs, corresponding to an effective optical path length of 6.7 km. Each ring-down measurement has a frequency resolution of 14 kHz (given by the FSR divided by the cavity finesse). The noise-equivalent absorption spectral density is 2.3×10^{-11} cm^{-1}Hz$^{-1/2}$ for both the L2130-*i* and L2130-*i*-C, and the L2140-*i* instruments. This corresponds to a noise-equivalent absorption of only 7×10^{-13} cm^{-1} for integration times of 10^3 s.

2.3.2 Spectroscopy

The use of laser-current tuning permits greater accuracy in the determination of the width of spectral lines than was achievable with the L2130-*i* or L2130-*i*-C instruments. This allows us, with the L2140-*i*, to use the integrated absorption under the spectral lines, rather than the height of spectral peaks, to determine isotopologue abundances (e.g., Kerstel, 2004; Kerstel et al., 2006; Hodges and Lisak, 2007).

The integrated absorption (cm^{-1}) is given by

$$A = u\int_0^\infty \kappa(\tilde{\nu})\mathrm{d}\tilde{\nu}, \tag{10}$$

where $\kappa(\tilde{\nu},T,P)$ is the molecular monochromatic absorption coefficient (cm^2), u is the column density of absorbers (cm^{-2}) and $\tilde{\nu}$ is the wavenumber (cm^{-1}) (Rothman et al., 1996).

The integrated absorption is directly related to the absorption strength, S, via

$$\kappa(\tilde{\nu},T,P) = S(T)\,f(\tilde{\nu},T,P), \tag{11}$$

where f is the line shape function due to Doppler and pressure spectral line broadening, T is temperature and P is pressure. The integral $\int_0^\infty f(\tilde{\nu},T,P)\mathrm{d}\tilde{\nu}=1$ and S is independent of pressure (Rothman et al., 1996). The ratios A_i/A_j for two different absorbing isotopologues i and j – and therefore in principle the isotope ratios – are also independent of pressure. This makes the integrated absorption superior to the spectral peak amplitude used in earlier-generation instruments. In practice, it is convenient to replace the wavenumber, $\tilde{\nu}$, in the integral with the dimensionless detuning $x = (\tilde{\nu}-\tilde{\nu}_0)/\sigma_D$, following Varghese and Hanson (1984), where $\tilde{\nu_0}$ is the center frequency of the absorption line, and σ_D is the Doppler width (half-width of the Gaussian Doppler-broadening profile at $1/e$ of the height).

Values of A are obtained by a least-squares fit of the measurements to an empirically determined spectral model. The spectral model describes the measured absorption as the sum of a baseline and molecular absorption lines. Free parameters in the baseline are an offset, slope and quadratic curvature term. The molecular absorption spectrum is modeled as the

superposition of Galatry profiles, which describe the shape function, f, for each spectral line. The Galatry profile, G, is given by the real part of the Fourier transform of the correlation function, Φ (Galatry, 1961):

$$G(x,y,z) = \frac{1}{\sqrt{\pi}}\mathrm{Re}\left\{\int_0^\infty \left[\Phi(y,z,\tau)e^{-ix\tau}\mathrm{d}\tau\right]\right\},$$
$$\Phi(y,z,\tau) = \exp\left(-y\tau + \frac{1}{2z^2}\left[1 - z\tau - e^{-z\tau}\right]\right), \quad (12)$$

where x is the frequency separation from the line center normalized by the Doppler width (as given above), y and z are collisional broadening and narrowing parameters, respectively, and τ is dimensionless time.

The parameters that determine the shape of the lines are obtained from spectra acquired by operating the analyzer in a fine-scan mode where ring-downs are acquired with a frequency spacing much smaller than the line width and using the wavelength monitor to determine the frequency axis. This determines the relationship between the collisional broadening and narrowing parameters, y and z, and the relationship between y for the "normal" water peak ($H_2{}^{16}O$) and the values of y for each of the isotopologues. The Doppler width is a known function of temperature (e.g., Galatry, 1961) and is therefore a fixed parameter. This leaves three or four free parameters needed to describe absorption for unknown samples in each spectral region: one y parameter and one value for the integrated absorption, A, for each independent isotopologue spectral line of interest (e.g., one each for the $H_2{}^{18}O$, $H_2{}^{16}O$ and HDO lines in the 7200 cm^{-1} wavenumber region).

2.3.3 Determination of isotope ratios

For the determination of δ^{18}O and δ^{17}O, the $^{18}O/^{16}O$ and $^{17}O/^{16}O$ ratios are obtained from the ratios of integrated absorptions of the rare isotopologues on the second laser to the integrated absorption of the common isotopologue on the first laser:

$$^{18}R = \frac{A(H_2{}^{18}O(11))}{A(H_2{}^{16}O(2))}, \quad (13)$$

$$^{17}R = \frac{A(H_2{}^{17}O(13))}{A(H_2{}^{16}O(2))}, \quad (14)$$

where $H_2{}^{18}O(11)$, $H_2{}^{16}O(2)$, etc. refer to the absorption lines shown in Fig. 1.

The raw (uncalibrated) δ^{18}O and δ^{17}O values are then obtained using the usual definition of δ:

$$\delta^{18}O^{\mathrm{raw}} = \frac{^{18}R}{^{18}R_{\mathrm{ref}}} - 1\,, \quad (15)$$

$$\delta^{17}O^{\mathrm{raw}} = \frac{^{17}R}{^{17}R_{\mathrm{ref}}} - 1\,, \quad (16)$$

where the value of R_{ref} is an instrument-specific estimate of the ratio of integrated absorption of $H_2{}^{17}O$ or $H_2{}^{18}O$ to that of $H_2{}^{16}O$ for the IAEA water standard, VSMOW. Values of δD are determined similarly using data from the first laser only:

$$^{2}R = \frac{A(\mathrm{HDO}(3))}{A(H_2{}^{16}O(2))}, \quad (17)$$

$$\delta D^{\mathrm{raw}} = \frac{^{2}R}{^{2}R_{\mathrm{ref}}} - 1\,. \quad (18)$$

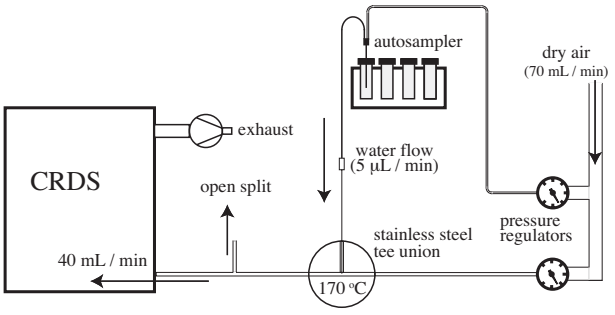

Figure 2. Schematic of custom vaporizer design used for isotope ratio measurements over long integration times. Double lines denote 1/16 inch and 1/32 inch stainless steel tubing (outside diameter). Single lines denote fused-silica capillary (0.3 mm inside diameter exiting the vials, reduced to 0.1 mm where the capillary enters the vaporizer).

2.4 Sample inlet system

We use two different inlet systems for the introduction of water into the CRDS optical cavity. To obtain measurements of the same water sample continuously over several hours, we use a "custom vaporizer". The custom vaporizer comprises a continuous-flow inlet system similar to that described by Gkinis et al. (2010, 2011) and used previously for δ^{18}O and δD. In this design, water is pumped continuously through a capillary and into a stainless steel tee union heated to 170 °C. In our application, the "pump" is a simple air pressure system, with a double needle that is used to puncture septum-sealed vials; air pressure introduced into the vial through a small steel tube pushes water through a fused-silica capillary and into the heated tee union. Within the tee union, the liquid water is mixed with dry air and exits the tee union as water vapor that is introduced into the CRDS optical cavity through an open split (Fig. 2). Water-vapor mixing ratios as measured by the CRDS analyzer are maintained at a target value (normally 20 mmol mol^{-1}) to within better than $\pm$0.1 mmol mol^{-1}.

For discrete injections of water into the CRDS we use a commercial vaporizer available from Picarro Inc. as model A0211 and described by Gupta et al. (2009). The vaporizer, operating at 110 °C, mixes dry carrier gas with 1.8 µL of water, which is injected through a septum. The resulting water vapor is introduced into the optical cavity via a three-way valve after a $\approx$ 60 s equilibration. Analysis of a single injection pulse takes approximately 120 s, excluding injection,

vaporizer purging and equilibration time. Automated sampling from 2 mL vials is accomplished with an autosampler (LEAP Technologies LC PAL). In our experiments, a complete vial analysis consists of 10 repeated injections from the same vial, for a total analysis time of about 1200 s.

3 Results

3.1 Measurement precision and drift

We use the custom vaporizer to obtain CRDS analyses of the isotope ratios of the same water over several hours. The Allan variance statistic provides a convenient way to assess the analytical precision and drift for the resulting long integrations. The Allan variance is defined as (Werle, 2011)

$$\sigma^2_{\mathrm{Allan}}(\tau_m) = \frac{1}{2\,\mathrm{m}} \sum_{j=1}^{m} \left(\overline{\delta}_{j+1} - \overline{\delta}_j\right)^2 , \qquad (19)$$

where τ_m is the integration time and $\overline{\delta}_{j+1}$, $\overline{\delta}_j$ are the mean values (e.g., $\delta = \delta^{18}\mathrm{O}$ or $\delta^{17}\mathrm{O}$) over neighboring time intervals. Here, we use the "Allan deviation" (σ_{Allan}, square root of the Allan variance) which can be interpreted as an estimate of the achievable reproducibility as a function of integration time.

Figure 3 shows σ_{Allan} for measurements made both with the L2130-*i*-C instrument using peak amplitudes, and with the L2140-*i* instrument using laser-current tuning and the integrated absorption measurement. In both cases, σ_{Allan} values for $\Delta^{17}\mathrm{O}$ of < 20 per meg are achieved after integration times of 5×10^2 s, and σ_{Allan} values for $\delta^{18}\mathrm{O}$, $\delta^{17}\mathrm{O}$ and $\delta\mathrm{D}$ are below 0.03, 0.03 and 0.04 ‰, respectively. However, these values represent the limits with the L2130-*i*-C; no additional improvements in precision were achieved with longer integration times, and in general σ_{Allan} begins to rise after 10^3 s. In contrast, with the L2140-*i*, σ_{Allan} values for $\delta^{18}\mathrm{O}$ and $\delta^{17}\mathrm{O}$ improve to < 0.015 ‰, and σ_{Allan} for $\Delta^{17}\mathrm{O}$ is better than 10 per meg after 1200 s (20 min). For $\delta\mathrm{D}$, the precision is < 0.07 ‰ at 10^3 s, and remains well below 0.1 ‰ for much longer integrations times ($> 10^4$ s). Both the measurements with the custom vaporizer, and those with the commercial vaporizer, show that long-term drift in $\Delta^{17}\mathrm{O}$ is greatly reduced in the L2140-*i*. Long-term drift for $\delta^{18}\mathrm{O}$ and $\delta^{17}\mathrm{O}$ is also improved, though not eliminated. We discuss the relationship between drift in $\delta^{18}\mathrm{O}$, $\delta^{17}\mathrm{O}$ and $\Delta^{17}\mathrm{O}$ in Sect. 4.

Repeated measurements of discrete water injections provide another way to assess measurement precision and drift. Results from running the same water from multiple vials (with 10 discrete 1.8 µL injections per vial), yield statistics comparable to those obtained with the custom vaporizer (Fig. 4). Typical injection-to-injection precision is 20 per meg for $\Delta^{17}\mathrm{O}$. Averages over 10 repeated injections from each vial result in a total analysis time per vial of 1200 s, corresponding to the integration time at which the Allan deviation data (Fig. 3) show $\Delta^{17}\mathrm{O}$ precision reaching < 10 per meg. Vial average reproducibility of $\Delta^{17}\mathrm{O}$ is 8 per meg. Typical vial-to-vial reproducibility is 0.03 ‰ for $\delta^{18}\mathrm{O}$, 0.015 ‰ for $\delta^{17}\mathrm{O}$, and 0.1 ‰ for $\delta\mathrm{D}$.

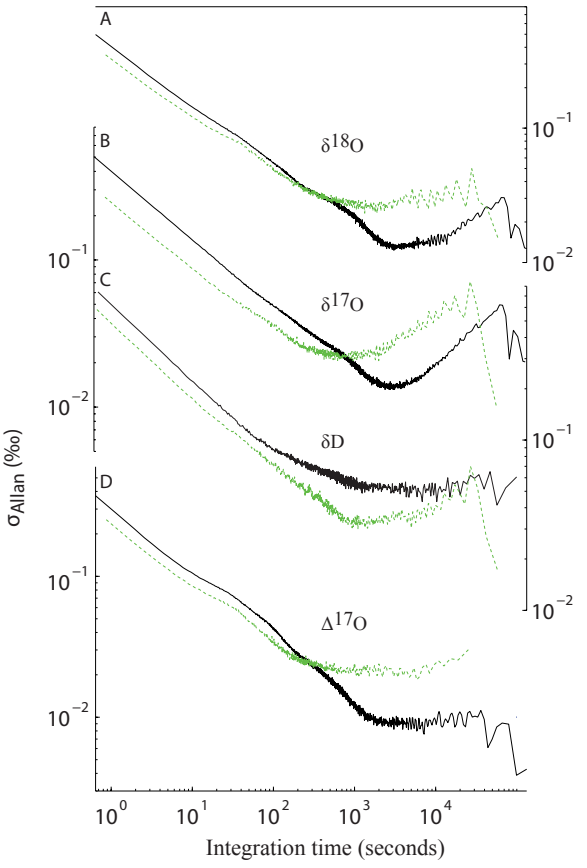

Figure 3. Comparison of Allan deviations for water isotope ratios with the L2130-*i*-C using a conventional wavelength monitor and spectral peak amplitude (green dashed lines), and with the L2140-*i* using laser-current-tuned cavity resonance and integrated absorption (solid lines). **(A)** $\delta^{18}\mathrm{O}$, **(B)** $\delta^{17}\mathrm{O}$, **(C)** $\delta\mathrm{D}$, **(D)** $\Delta^{17}\mathrm{O}$.

3.2 Sensitivity to water-vapor mixing ratio

Laser spectroscopy instruments used for water isotope measurements exhibit dependence of $\delta^{18}\mathrm{O}$ and $\delta\mathrm{D}$ values on the water-vapor mixing ratio (Gkinis et al., 2010), and similar dependence is expected for $\delta^{17}\mathrm{O}$ and $\Delta^{17}\mathrm{O}$. This dependence arises primarily from the effect of pressure broadening on peak shape. As noted in Sect. 2.3.2, use of the integrated absorption in place of peak amplitude in the calculation of isotope ratios with the L2140-*i* instrument should theoretically eliminate the water-vapor mixing-ratio dependence. We used the custom vaporizer to obtain measurements with the L2140-*i* over a wide range of water-vapor mixing ratios. Figure 5 shows that there is a significant reduction in the sensitivity of isotope ratios to mixing ratio when using the integrated absorption measurement, as

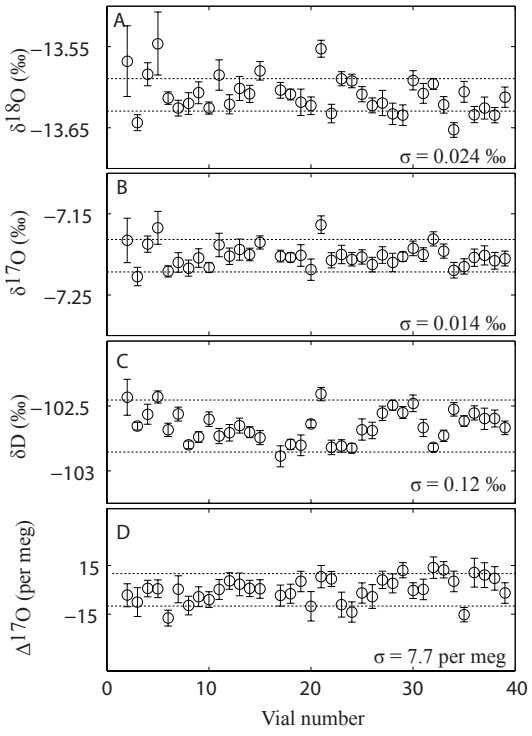

Figure 4. Isotope ratios from repeated measurements of 2 mL vials of identical water, using integrated absorption on the L2140-*i*. **(A)** δ^{18}O, **(B)** δ^{17}O, **(C)** δD, and **(D)** Δ^{17}O. Each dot represents the average of ten 1.8 µL injections from one vial; the vertical error bars show the standard error ($\sigma/\sqrt{n}$) of the $n = 10$ individual injections. The standard deviation of all vial means (σ) is given in each panel. Horizontal dashed lines are shown for reference at ±0.02 ‰ for δ^{18}O and δ^{17}O, at ±0.2 ‰ for δD, and at ±10 per meg for Δ^{17}O. The experiment shown took about 60 h. No drift corrections or other post-measurement adjustments were made to the raw data.

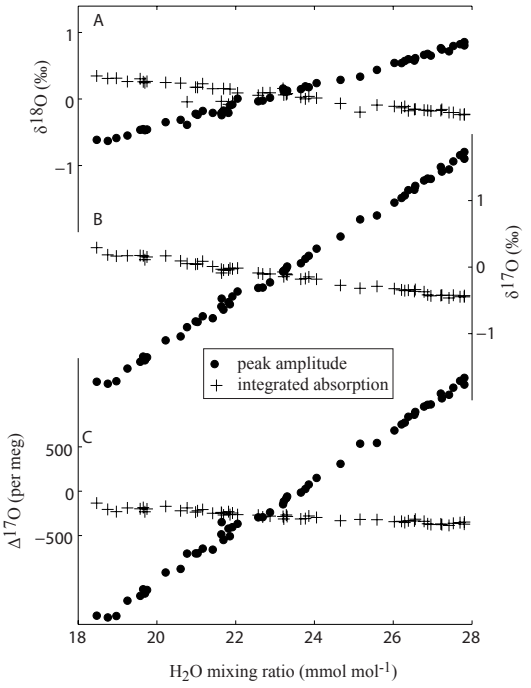

Figure 5. Comparison of the sensitivity of isotope ratio measurements on the L2140-*i* CRDS analyzer to the water-vapor mixing ratio using peak amplitude vs. integrated absorption. Note that a mixing ratio of 20 mmol mol^{-1} is reported by the instrument software as a concentration (20 000 ppm). **(A)** δ^{18}O, **(B)** δ^{17}O and **(C)** Δ^{17}O.

expected. For δ^{18}O, sensitivity is reduced from 0.2 ‰ for a 1 mmol mol^{-1} variation in water-vapor mixing ratio – comparable to that seen in the L2130-*i* and other earlier-generation instruments – to less than 0.04 ‰/(mmol mol^{-1}). Sensitivity for δ^{17}O is comparably reduced, from 0.4 ‰ to less than 0.08 ‰/(mmol mol^{-1}). Finally, the sensitivity of Δ^{17}O to the water-vapor mixing ratio is reduced from > 250 per meg to < 30 per meg/(mmol mol^{-1}). The mixing-ratio sensitivity of δD, however, at about 1 ‰/(mmol mol^{-1}) is not significantly changed between earlier models and the L2140-*i*. This may suggest an incomplete accounting for the structure of the mixing-ratio-dependent spectral baseline, or other aspects of the spectroscopy that are not yet fully characterized.

3.3 Calibration to VSMOW and SLAP

We performed two independent types of calibration experiments with the L2140-*i*. In the first experiment, we analyzed standard waters SLAP2 and VSMOW2, along with reference waters GISP, VW (Vostok Water), WW (West Antarctic Ice Sheet Water) and KD (Kona Deep), and used the two-point calibration lines defined by Eqs. (7) and (8) to determine the value of the references waters treated as "unknowns". The resulting calibrated δ^{18}O and δ^{17}O values are then used to calculate Δ^{17}O, using Eq. (5) (note that the δ^{18}O and δ^{17}O of VSMOW2 and SLAP2 are indistinguishable from those of VSMOW and SLAP (Lin et al., 2010)). In the second experiment, we analyzed lab reference waters SW (Seattle Water) and WW and used the IRMS δ^{18}O and δ^{17}O values of PW (Pennsylvania Water) and VW as calibration points.

In both types of calibration experiments, we used the commercial vaporizer and 2 mL vials, from which ten 1.8 µL injections were made. The measurement order was as follows, where the number gives the number of vials for each water sample in parentheses. First experiment: 5 (KD), 5 (VSMOW2), 4 (VW), 5 (SLAP2), 4 (WW), 5 (GISP), 5 (KD), 5 (VSMOW2), 4 (WW), 5 (GISP), 4 (VW), and 5 (SLAP2). Second experiment: 7 (VW), 7 (WW), 7 (SW), 7 (KD), 7 (PW), 7 (VW), 7 (WW), 7 (SW), 7 (KD), and

7 (PW). In the experiment with VSMOW2, SLAP2 and GISP, the use of lab reference waters with similar isotopic composition prior to the IAEA standards was done in order to reduced the potential for instrument memory effects influencing the results. We use data only from the last three vials for each standard or reference water in our calculations, using all 10 injections from each of those vials in the average. We find that the instrument response time for δ^{17}O is indistinguishable from that for δ^{18}O. This suggests that memory effects should be minimized for Δ^{17}O measurements compared with deuterium excess, which can be problematic because the response time for δD is greater than for δ^{18}O in most instruments (Aemisegger et al., 2012). Further work is needed, however, to fully characterize the influence of memory on Δ^{17}O with the L2140-*i*.

The results of the calibration experiments are tabulated in Table 2. Figure 6 shows the calibrated mean values and uncertainties in Δ^{17}O for the two different types of calibration experiment. The uncertainties are calculated as the standard deviation of the mean ($\sigma/\sqrt{n}$) based on n repeated measurements. This calculation may underestimate the true uncertainty because it assumes a Gaussian error distribution, which is not supported by the Allan deviation data for long integration times (Fig. 3). However, this is conservative with respect to the calibration experiments: the results show that the Δ^{17}O values of the "unknowns" in each experiment with the CRDS are indistinguishable from the values previously determined using IRMS. Note in particular that the CRDS value of the IAEA reference water, GISP (27 ± 4 per meg), calibrated independently, is nearly identical to the IRMS value of 28 ± 2 per meg (Schoenemann et al., 2013). Further, we find that both KD, which is fresh water derived by reverse osmosis from an ocean water sample, and VW, which is a meteoric water sample from the interior of East Antarctica, have indistinguishable Δ^{17}O values.

We emphasize that, as with IRMS measurements, data that are referenced to VSMOW but are not normalized on the VSMOW-SLAP scale can result in inconsistent results because of instrument-specific scale compression (or expansion) relative to the defined calibration (see e.g., Coplen, 1988; Schoenemann et al., 2013). In the context of Δ^{17}O measurements on water, such scale compression results in a slope differing from the defined value of 0.528 on a plot of $\ln(\delta^{17}\mathrm{O}+1)$ vs. $\ln(\delta^{18}\mathrm{O}+1)$. Also, if the slope is significantly different from 0.528, errors in Δ^{17}O will result even if a linear normalization to VSMOW-SLAP is applied. This problem can in principle be addressed using a nonlinear normalization method (Kaiser, 2008); i.e.,

$$\delta^{17}\mathrm{O}_{\mathrm{sample}}^{\mathrm{normalized}} = (\delta^{17}\mathrm{O}_{\mathrm{sample}}^{\mathrm{measured}}+1)^{\frac{\ln((\delta^{17}\mathrm{O}_{\mathrm{SLAP}}^{\mathrm{assigned}}+1))}{\ln((\delta^{17}\mathrm{O}_{\mathrm{SLAP}}^{\mathrm{measured}}+1)}} - 1\,, \quad (20)$$

and similarly for δ^{18}O, rather than our linear calculation (Eqs. 7–9). However, the nonlinear calibration method cannot effectively remove scale compression due to blank

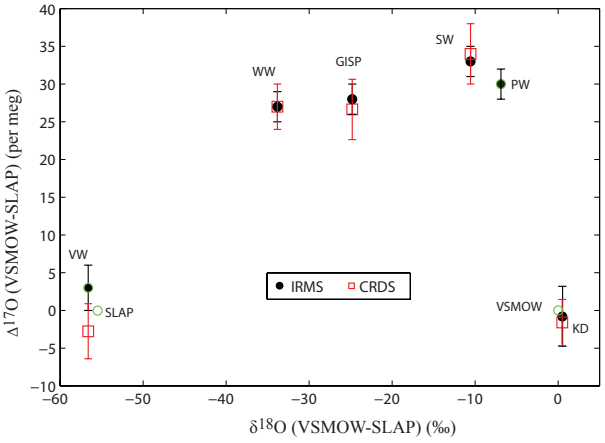

Figure 6. Comparison of Δ^{17}O data from two independent sets of calibrations of reference waters and standards measured by laser spectroscopy on the L2140-*i* (CRDS, open squares) with previously determined values from mass spectrometry (IRMS, filled circles). Δ^{17}O data are plotted vs. δ^{18}O. Error bars on the CRDS values are the standard deviation of the mean (see Table 2). Values and error bars (1 standard error) on the IRMS values are from Table 1, updated from Schoenemann et al. (2013). The calibration points VSMOW, SLAP, PW and VW are shown as open circles for reference.

effects. In our case, as shown in Fig. 7, the slope of $\ln(\delta^{17}\mathrm{O}+1)$ vs. $\ln(\delta^{18}\mathrm{O}+1)$ is 0.5254; the scale compression is therefore 0.995. Use of Eq. (20) would result in a difference for the GISP reference water of < 0.0006‰ for δ^{17}O, < 0.003‰ for δ^{18}O and < 1.6 per meg for Δ^{17}O, all well below measurement uncertainty. Use of the linear normalization from Schoenemann et al. (2013) is therefore preferred. Nevertheless, users of L2140-*i* instruments will need to verify any calibration strategy for their particular application, taking into account the instrument response time, the availability of reference waters of known composition, and the scale compression, which may be different for different instruments.

4 Discussion

Our results demonstrate that analysis of Δ^{17}O using cavity ring-down laser absorption spectroscopy, as implemented in the L2140-*i* instrument, can be competitive with analyses by mass spectrometry. The reproducibility of repeated individual measurements made over 30 min is better than 8 per meg, similar to the precision reported for IRMS (e.g., Luz and Barkan, 2010; Schoenemann et al., 2013), and calibrated values of reference waters are indistinguishable between the two methods. Achieving Δ^{17}O measurements at the < 10 per meg level with CRDS requires relatively long integration times when compared with the more common δ^{18}O or δD measurements, which for typical applications require lower

Table 2. VSMOW-SLAP-normalized $\Delta^{17}O$, $\delta^{18}O$, $\delta^{17}O$ and δD values for reference waters determined by CRDS using (a) IAEA standards VSMOW2 and SLAP2 as calibration points and (b) using University of Washington standards PW and VW as calibration points. IRMS-measured $\Delta^{17}O$ values are shown for comparison. Precision ($\pm$) is the standard deviation of the mean ($\sigma/\sqrt{n}$). n is the sample size.

	IRMS $\Delta^{17}O$ (per meg)	CRDS $\Delta^{17}O$ (per meg)	$\delta^{18}O$ (‰)	$\delta^{17}O$ (‰)	δD (‰)	n
GISP[a]	28 ± 2	27 ± 4	-24.77 ± 0.02	-13.13 ± 0.01	-190.19 ± 0.14	6
VW[a]	3 ± 3	-3 ± 3	-56.50 ± 0.03	-30.24 ± 0.02	-438.19 ± 0.35	6
WW[a]	27 ± 2	27 ± 4	-33.90 ± 0.03	-18.02 ± 0.02	-268.87 ± 0.40	6
WW[b]	27 ± 2	27 ± 2	-33.98 ± 0.03	-18.06 ± 0.03	-269.29 ± 0.26	6
SW[b]	33 ± 2	34 ± 4	-10.64 ± 0.04	-5.60 ± 0.03	-76.05 ± 0.24	6
KD[a]	-0.8 ± 4	-1.6 ± 3	0.43 ± 0.01	0.23 ± 0.01	1.33 ± 0.13	6
KD[b]	-0.8 ± 4	-1.6 ± 4	0.50 ± 0.03	0.26 ± 0.03	1.71 ± 0.22	6

[a] VSMOW2 and SLAP2 calibration. [b] PW and VW calibration. Errors take into account uncertainty in calibration points.

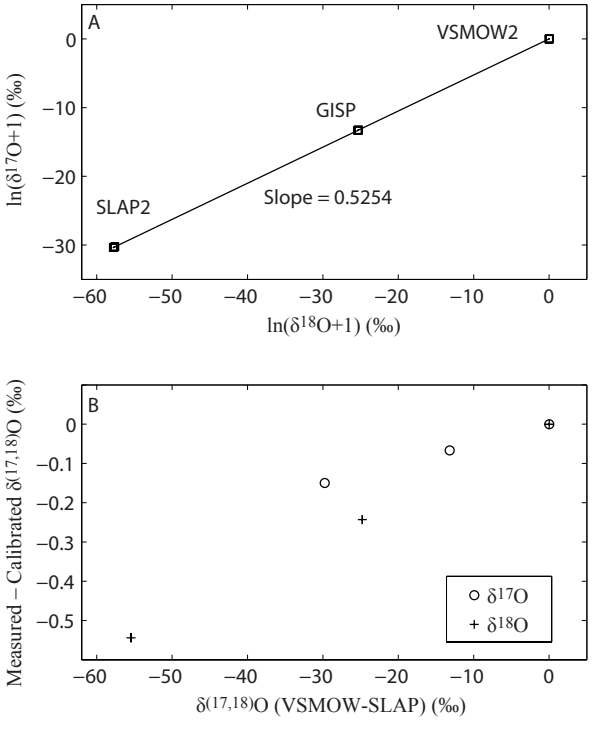

Figure 7. Characterization of scale compression on the L2140-*i*. **(A)** Measured (vs. VSMOW) $\ln(\delta^{17}O + 1)$ vs. $\ln(\delta^{18}O + 1)$ for VSMOW2, SLAP2 and GISP. **(B)** Difference between measured and calibrated $\delta^{17}O$ and $\delta^{18}O$ of VSMOW2, SLAP2 and GISP as a function of the calibrated value.

precision (< 0.1 and < 1‰, respectively). Nevertheless, the new method is less time consuming, less labor intensive, and safer than the IRMS method requiring the use of fluorination.

Measurements of $\Delta^{17}O$ with a laser spectroscopy instrument with a different design (off-axis integrated cavity output spectroscopy, or OA-ICOS) were reported recently by Berman et al. (2013). Measurements of the IAEA reference water GISP reported by Berman et al. (2013), when calibrated to VSMOW and SLAP, are somewhat lower than ours (23 ± 2 per meg, compared with our values of 27 ± 4 (CRDS) and 28 ± 2 (IRMS)), but both are compatible within 2σ of most reported IRMS values from the literature; e.g., the weighted average of the most precise previously reported measurements (IRMS only) was 22 ± 11 per meg (Schoenemann et al., 2013). The mean VSMOW-SLAP-normalized value for GISP for all recent measurements from four different laboratories (as reported here, and by Schoenemann et al., 2013 and Berman et al., 2013) is $\Delta^{17}O = 28 \pm 3$ per meg.

High-precision $\Delta^{17}O$ measurements are achieved without drift correction on the L2140-*i*. Indeed, the precision and drift characteristics of the $\Delta^{17}O$ results are better than would be expected from the simple combination of noise in the $\delta^{18}O$ and $\delta^{17}O$ measurements, both of which show evidence of some drift in their Allan deviations (Fig. 3).

The relationship between $\delta^{18}O$, $\delta^{17}O$ and $\Delta^{17}O$ errors can be understood as a combination of correlated and uncorrelated noise contributions (Schoenemann et al., 2013):

$$\sigma_{xs} = (m - 0.528)\sigma_{18} + \eta_{17} \,, \quad (21)$$

where σ_{xs} is the precision of $\Delta^{17}O$, σ_{18} is the precision of $\ln(\delta^{18}O+1)$, and η_{17} is the residual in $\ln(\delta^{17}O + 1)$ from a best-fit line through the data having slope m. In general, the uncorrelated errors (η_{17}) are small. At higher frequencies, m tends towards higher values (Fig. 8).

We find that for the 0.8 s averages of ≈ 400 individual ring-down measurements, the slope is 0.82 ± 0.02, or 1.0 ± 0.1 if a "model 2" regression that accounts for variance in both the $\delta^{18}O$ and $\delta^{17}O$ measurements is used (e.g., York, 1969). A slope of precisely 1.0 would be expected if, for example, all measurement error were due to noise in the $H_2{}^{16}O$ spectral line, since this measurement is shared equally in the calculation of both $\delta^{18}O$ and $\delta^{17}O$. The noise in the high-

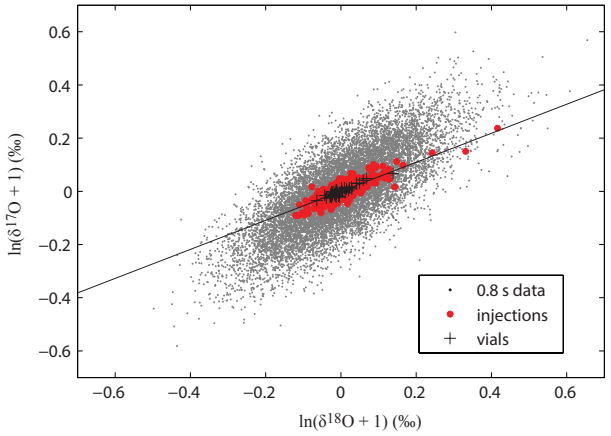

Figure 8. Relationship between $\ln(\delta^{17}\mathrm{O}+1)$ and $\ln(\delta^{18}\mathrm{O}+1)$ residuals for 40 vials of identical water, each injected 10 times in the L2140-*i* CRDS. Small gray dots show every 100th high-frequency 0.8 s measurement, large circles the individual injection means,"+"-signs the vial-mean values. The slopes of the 0.8 s and individual injection data are 0.82 ± 0.02 and 0.59 ± 0.02, respectively ($\pm = 2\sigma$). The slope of the vial-mean data is 0.54 ± 0.03, shown by the line.

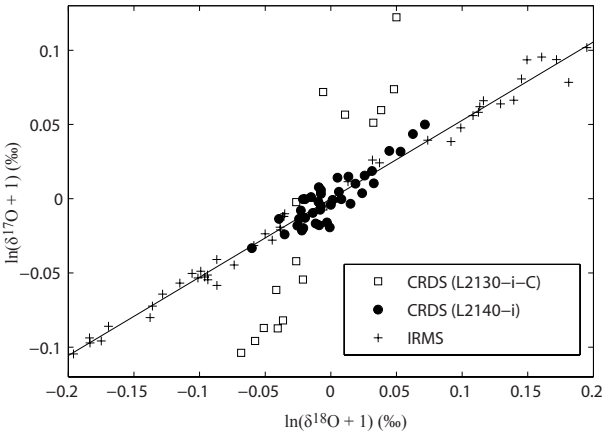

Figure 9. Comparison of the $\ln(\delta^{17}\mathrm{O}+1)$ vs. $\ln(\delta^{18}\mathrm{O}+1)$ relationship for residuals (difference of individual analyses from the mean) of measurements of water samples with the L2130-*i*-C and the L2140-*i* CRDS instruments, and with IRMS. The slope of 0.528 that defines Δ^{17}O is shown for reference.

frequency data is indistinguishable from Gaussian, and is consequently reduced as a function of the square root of the integration time. For longer measurement times (integrations of 10^3 s or longer), m is ≈ 0.5, so that the term $(m-0.528)\sigma_{18}$ is small. As for IRMS measurements, it is the combination of the very small magnitude of uncorrelated noise, η_{17}, combined with $m \approx 0.5$ that leads to the very high precision for Δ^{17}O measurements, even where the δ^{18}O and δ^{17}O measurements are comparatively imprecise.

Frequency dependence of the error slope, m, is not observed in IRMS measurements. As discussed in Schoenemann et al. (2013), in both the H_2O fluorination procedure and in the mass-spectrometer source, likely sources of error will involve some combination of diffusive and equilibrium fractionation processes, both of which will lead to values of m close to 0.5 (e.g., Miller, 2002). That the relationship between δ^{18}O and δ^{17}O errors in the CRDS also tends towards $m \approx 0.5$ at longer integration times suggests that low-frequency drift in these measurements is similarly attributable to fractionation effects, rather than, for example, drift in the optical cavity temperature or other aspects of the CRDS instrument itself. Fractionation of the δ^{18}O and δ^{17}O values could be associated with diffusion of water vapor, incomplete evaporation, or condensation and re-evaporation during the vaporization process, or possibly in the optical cavity.

These observations suggest that the current practical limit of precision for isotope measurements on the L2140-*i* is set by the sample introduction system, rather than the CRDS analysis itself. As illustrated in Fig. 9, which compares IRMS and CRDS measurements, the magnitude of η_{17} is very small – similar to that obtained with high-precision IRMS – while the magnitude of σ_{18} is much smaller than that obtained with IRMS measurements of O_2 prepared by fluorination.

This was not the case with our original prototype instrument (L2130-*i*-C), for which analyzer noise was dominant even for long integration times (Fig. 9). Because the term $(m-0.528)\sigma_{18}$ is very small, < 1 per meg, for vial-average measurements, changes to the sample introduction system that would significantly improve Δ^{17}O precision will be challenging. These comparisons attest to the significant improvement in the spectroscopic measurements achieved in the L2140-*i*, as well as to the stability of the water-vapor delivery and minimal amount of fractionation occurring both in the commercial vaporizer and in our custom vaporizer design.

The L2140-*i* should be useful in a variety of applications, such as the high-resolution analysis of ice core samples using in-line continuous melting systems (Gkinis et al., 2011), or in the measurement of ambient water-vapor mixing ratios in the atmosphere, currently done with laser spectroscopy instruments for δ^{18}O and δD (e.g., Noone et al., 2011; Sayres et al., 2009), though such applications have not yet been fully tested. The low sensitivity to water-vapor mixing ratio achieved with the integrated-absorption measurement would be an advantage in such applications, though there is still some sensitivity that may become important for mixing-ratio variability greater than ± 0.1 mmol mol^{-1}. In the current commercial version of the L2140-*i* instrument, a water-vapor mixing-ratio correction is available in the instrument software that uses a bilinear relationship of the form

$$A(1)_{\mathrm{corrected}} = A(1) + a_0 + a_1 A(1) A(2), \qquad (22)$$

where $A(1)$ and $A(2)$ refer to the integrated absorption for peaks 1 and 2 (Fig. 1), and a_0 and a_1 are empirically determined coefficients. The coefficients are determined by

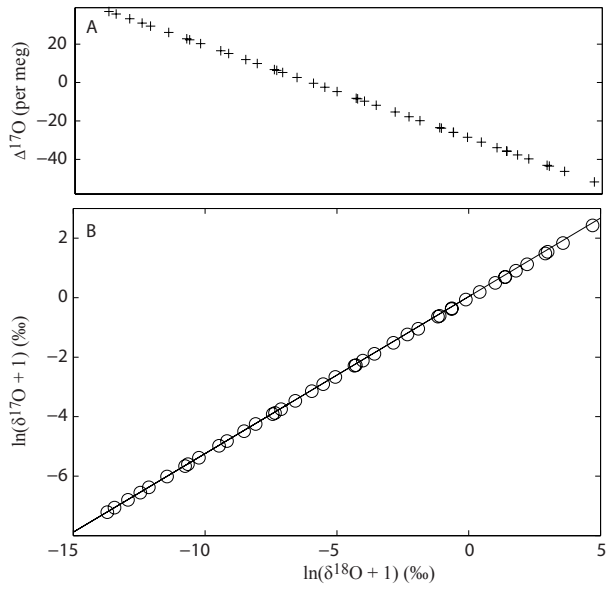

Figure 10. Results of an evaporation experiment in which 2 mL sample vials are left open to the ambient air and are progressively sampled (ten 1.8 µL injections for each vial) over a ≈ 60 h period. **(A)** δ^{17}O vs. $\ln(\delta^{18}\mathrm{O}+1)$, **(B)** $\ln(\delta^{17}\mathrm{O}+1)$ vs. $\ln(\delta^{18}\mathrm{O}+1)$. Time progress to the right in both panels. Note the gradual deviation of the measurements (open circles) from a slope of 0.528 (line).

varying the water mixing ratio over a large range and then applied to each measurement. A similar correction is applied to $A(3)$, $A(11)$, and $A(13)$. A simple linear correction following instrument-specific empirical measurements such as illustrated in Fig. 5 could be used as an alternative. We note, however, that we have not evaluated the performance of the instrument at low water-vapor mixing ratios (< 18 mmol mol^{-1}).

As an example of an application of the L2140-*i*, we performed a simple experiment in which 42 vials containing identical water, open to the air, were measured sequentially using 10 injections each. Because the vials were open to a relatively low-humidity laboratory atmosphere, evaporation of the vials would be expected to raise the δ^{18}O values through time, and the Δ^{17}O value should decrease; furthermore, the relationship between $\ln(\delta^{17}\mathrm{O}+1)$ and $\ln(\delta^{18}\mathrm{O}+1)$ would be expected to evolve along a slope intermediate between the equilibrium value (0.529) (Barkan and Luz, 2005) and the value for diffusion into dry air (0.518) (Barkan and Luz, 2007). These features are indeed observed in the experiment: Δ^{17}O decreases by 90 per meg (Fig. 10).

The slope of $\ln(\delta^{17}\mathrm{O}+1)$ vs. $\ln(\delta^{18}\mathrm{O}+1)$ is 0.5232 ± 0.0005, distinguishable at $> 99\%$ confidence from the "meteoric water line" slope, accounting for scale compression. A simple experiment like this, which was run fully automated over ≈ 60 h, would take many hours of sample preparation time and > 100 h of analysis time using the traditional fluorination and IRMS method. Note also that the progressive lowering of the Δ^{17}O value is clearly detectable from vial to vial at the 1–2 per meg level; this would probably not be possible to observe using the IRMS method. We suggest that the laser spectroscopy method for Δ^{17}O could be used in a number of hydrological and atmospheric sciences applications that were previously impractical.

5 Conclusions

CRDS is commonly used for measurements of the ^{18}O / ^{16}O and D / H isotope ratios of water and water vapor, reported as δ^{18}O and δD deviations from VSMOW. We have developed a new CRDS instrument that makes possible the additional measurement of the ^{17}O/^{16}O isotope ratio, and of the small difference, Δ^{17}O, between $\ln(\delta^{17}\mathrm{O}+1)$ and $0.528\ln(\delta^{18}\mathrm{O}+1)$, known as the "^{17}O excess". The new instrument uses a novel laser-current-tuned cavity resonance method to achieve precision of < 8 per meg for Δ^{17}O while simultaneously providing measurements of δ^{18}O and δD with a precision competitive with previous-generation instruments. Liquid samples are introduced into the optical cavity using an automated vaporization system that requires no prior sample preparation. Direct analysis of ambient water vapor in air is also possible. Calibration against the IAEA standard waters VSMOW2 and SLAP2 yields calibrated values for the reference water GISP of 27 ± 4 per meg, indistinguishable from the value of 28 ± 2 obtained by Schoenemann et al. (2013) using IRMS. Our results establish CRDS measurements of Δ^{17}O of H_2O as a viable alternative to conventional IRMS methods that require the use of fluorination to convert H_2O samples to O_2 prior to analysis.

Acknowledgements. We thank B. Vanden Heuvel, B. H. Vaughn, J. W. C. White, B. Vinther, G. Hsiao and E. Crosson. Reviews by E. Kerstel, J. Kaiser and E. Berman led to improvements in the manuscript. We also thank the editor for his handling of the manuscript. This work was supported by the US National Science Foundation Division of Polar Programs (Antarctic Glaciology Program), Division of Atmospheric and Geospace Sciences (Paleoclimate Program; Climate and Large Scale Dynamics Program) and Division of Industrial Innovation & Partnerships (Academic Liaison with Industry Program) (NSF award numbers DPP-1341360 and OPP-0806387). It was also supported by the Quaternary Research Center at the University of Washington, the Centre for Ice and Climate at the University of Copenhagen, and the Lundbeck Foundation, Copenhagen, Denmark.

Edited by: D. Heard

References

Abe, O.: Isotope fractionation of molecular oxygen during adsorption/desorption by molecular sieve zeolite, Rapid Commun. Mass Spec., 22, 2510–2514, 2008.

Aemisegger, F., Sturm, P., Graf, P., Sodemann, H., Pfahl, S., Knohl, A., and Wernli, H.: Measuring variations of δ^{18}O and δ^{2}H in atmospheric water vapour using two commercial laser-based spectrometers: an instrument characterisation study, Atmos. Meas. Tech., 5, 1491–1511, doi:10.5194/amt-5-1491-2012, 2012.

Audi, G., Wapstra, A. H., and Thibault, C.: The 2003 atomic mass evaluation. II: Tables, graphs and references, Nucl. Phys. A, 729, 337–676, 2003.

Baker, L., Franchi, I. A., Maynard, J., Wright, I. P., and Pillinger, C. T.: A technique for the determination of ^{18}O/^{16}O and ^{17}O/^{16}O isotopic ratios in water from small liquid and solid samples, Anal. Chem., 74, 1665–1673, 2002.

Barkan, E. and Luz, B.: High precision measurements of ^{18}O/^{16}O and ^{17}O/^{16}O ratios in H_2O, Rapid Commun. Mass Sp., 19, 3737–3742, 2005.

Barkan, E. and Luz, B.: Diffusivity fractionations of $H_2{}^{16}O/H_2{}^{17}O$ and $H_2{}^{16}O/H_2{}^{18}O$ in air and their implications for isotope hydrology, Rapid Commun. Mass Spec., 21, 2999–3005, 2007.

Begley, I. S. and Scrimgeour, C. M.: High-precision δ^{2}H and δ^{18}O measurement for water and volatile organic compounds by continuous-flow pyrolysis isotope ratio mass spectrometry, Anal. Chem., 69, 1530–1535, 1997.

Berman, E. S. F., Levin, N., Landais, A., Li, S., and Thomas Owano, T.: Measurement of δ^{18}O, δ^{17}O, and ^{17}O-excess in water by off-axis integrated cavity output spectroscopy and isotope ratio mass spectrometry, Anal. Chem., 85, 10392–10398, 2013.

Bigeleisen, J., Perlman, M. L., and Prosser, H. C.: Conversion Of hydrogenic materials to hydrogen for isotopic analysis, Anal. Chem., 24, 1356–1357, 1952.

Blossey, P. N., Kuang, Z., and Romps, D. M.: Isotopic composition of water in the tropical tropopause layer in cloud-resolving simulations of an idealized tropical circulation, J. Geophys. Res.-Atmos., 115, D24309, doi:10.1029/2010JD014554, 2010.

Brand, W. A., Geilmann, H., Crosson, E. R., and Rella, C. W.: Cavity ring-down spectroscopy versus high-temperature conversion isotope ratio mass spectrometry; a case study on δ^{2}H and δ^{18}O of pure water samples and alcohol/water mixtures, Rapid Commun. Mass Spec., 23, 1879–1884, 2009.

Cohn, M. and Urey, H.: Oxygen exchange reactions of organic compounds and water, J. Am. Chem. Soc., 60, 679–687, 1938.

Coplen, T.: Normalization of oxygen and hydrogen isotope data, Chem. Geol., 72, 293–297, 1988.

Craig, H. H.: Isotopic standards for carbon and oxygen and correction factors for mass-spectrometric analysis of carbon dioxide, Geochim. Cosmochim. Acta, 12, 133–149, 1957.

Crosson, E. R.: A cavity ring-down analyzer for measuring atmospheric levels of methane, carbon dioxide, and water vapor, Appl. Phys. B, 92, 403–408, 2008.

Crosson, E., Fidric, B., Paldus, B., and Tan, S.: Wavelength control for cavity ringdown spectrometer, Patent US7106763 B2, Picarro, Inc., 2006.

Dansgaard, W.: Stable isotopes in precipitation, Tellus, 16, 436–468, 1964.

Dansgaard, W., Clausen, H., Gundestrup, N., Hammer, C., Johnsen, S., Kristinsdottir, P., and Reeh, N.: A new Greenland deep ice core, Science, 218, 1273–1277, 1982.

Epstein, S. and Mayeda, T.: Variations of ^{18}O content of waters from natural sources, Geochim. Cosmochim. Acta, 4, 213–224, 1953.

Galatry, L.: Simultaneous effect of Doppler and foreign gas broadening on spectral lines, Phys. Rev., 122, 1218–1223, 1961.

Gehre, M., Hoefling, R., Kowski, P., and Strauch, G.: Sample preparation device for quantitative hydrogen isotope analysis using chromium metal, Anal. Chem., 68, 4414–4417, 1996.

Gehre, M., Geilmann, H., Richter, J., Werner, R. A., and Brand, W. A.: Continuous flow ^{2}H/^{1}H and ^{18}O/^{16}O analysis of water samples with dual inlet precision, Rapid Commun. Mass Spec., 18, 2650–2660, 2004.

Gianfrani, L., Gagliardi, G., van Burgel, M., and Kerstel, E. R. T.: Isotope analysis of water by means of near-infrared dual-wavelength diode laser spectroscopy, Opt. Express, 11, 1566–1576, 2003.

Gkinis, V., Popp, T. J., Johnsen, S. J., and Blunier, T.: A continuous stream flash evaporator for the calibration of an IR cavity ring-down spectrometer for the isotopic analysis of water, Isotop. Environ. Health Stud., 46, 463–475, 2010.

Gkinis, V., Popp, T. J., Blunier, T., Bigler, M., Schüpbach, S., Kettner, E., and Johnsen, S. J.: Water isotopic ratios from a continuously melted ice core sample, Atmos. Meas. Tech., 4, 2531–2542, doi:10.5194/amt-4-2531-2011, 2011.

Gonfiantini, R.: Standards for stable isotope measurements in natural compounds, Nature, 271, 534–536, 1978.

Gonfiantini, R., Stichler, W., and Rozanski, K.: Standards and Intercomparison Materials Distributed by the International Atomic Energy Agency for Stable Isotope Measurements, Vol. 825 of IAEA-TECDOC, 13–29, International Atomic Energy Agency, Vienna, 1995.

Gupta, P., Noone, D., Galewsky, J., Sweeney, C., and Vaughn, B. H.: Demonstration of high-precision continuous measurements of water vapor isotopologues in laboratory and remote field deployments using wavelength-scanned cavity ring-down spectroscopy (WS-CRDS) technology, Rapid Commun. Mass Spec., 23, 2534–2542, 2009.

Hsiao, G. Hoffnagle, J. Gkinis, V., Steig, E. J., Vaughn, B., Schoenemann, S. and Schauer, A: $^{17}O_{excess}$ measurements of water without fluorination using optical spectroscopy, Geophysical Research Abstracts, 14, EGU2012-6565, 2012.

Hodges, J. T. and Lisak, D.: Frequency-stabilized cavity ring-down spectrometer for high-sensitivity measurements of water vapor concentration, Appl. Phys. B., 85, 375–382, 2007.

Johnsen, S. J., Dansgaard, W., and White, J. W. C.: The origin of Arctic precipitation under present and glacial conditions, Tellus B, 41, 452–468, 1989.

Johnsen, S. J., Clausen, H. B., Dansgaard, W., Gundestrup, N. S., Hammer, C. U., and Tauber, H.: The Eem stable-isotope record along the GRIP ice core and its interpretation, Quaternary Res., 43, 117–124, 1995.

Jouzel, J., Masson-Delmotte, V., Cattani, O., Dreyfus, G., Falourd, S., Hoffmann, G., Minster, B., Nouet, J., Barnola, J. M., Chappellaz, J., Fischer, H., Gallet, J. C., Johnsen, S., Leuenberger, M., Loulergue, L., Luethi, D., Oerter, H., Parrenin, F., Raisbeck, G., Raynaud, D., Schilt, A., Schwander, J., Selmo, E., Souchez, R., Spahni, R., Stauffer, B., Steffensen, J. P., Stenni, B., Stocker, T. F., Tison, J. L., Werner, M., and Wolff, E. W.: Orbital and millennial Antarctic climate variability over the past 800 000 years, Science, 317, 793–796, 2007.

Kaiser, J.: Reformulated ^{17}O correction of mass spectrometric stable isotope measurements in carbon dioxide and a critical appraisal of historic "absolute" carbon and oxygen isotope ratios, Geochim. Cosmochim. Acta, 72, 1312–1334, 2008.

Kerstel, E. R. T.: Isotope ratio infrared spectrometry, Vol. 1 of Handbook of Stable Isotope Analytical Techniques, 759–787, Elsevier B. V., Amsterdam, 2004.

Kerstel, E. R. T., van Trigt, R., Dam, N., Reuss, J., and Meijer, H. A. J.: Simultaneous determination of the ^{2}H/^{1}H, ^{17}O/^{16}O and ^{18}O/^{16}O isotope abundance ratios in water by means of laser spectrometry, Anal. Chem., 71, 5297–5303, 1999.

Kerstel, E. R. T., Gagliardi, G., Gianfrani, L., Meijer, H. A. J., van Trigt, R., and Ramaker, R.: Determination of the ^{2}H/^{1}H, ^{17}O/^{16}O, and ^{18}O/^{16}O isotope ratios in water by means of tunable diode laser spectroscopy at 1.39 µm, Spectrochim. Ac. A, 58, 2389–2396, 2002.

Kerstel, E. R. T., Iannone, R. Q., Chenevier, M., Kassi, S., Jost, H. J., and Romanini, D.: A water isotope (^{2}H, ^{17}O, ^{18}O) spectrometer based on optical feedback cavity-enhanced absorption for in situ airborne applications, Appl. Phys. B, 85, 397–406, 2006.

Kurita, N., Newman, B. D., Araguas-Araguas, L. J., and Aggarwal, P.: Evaluation of continuous water vapor δD and δ^{18}O measurements by off-axis integrated cavity output spectroscopy, Atmos. Meas. Tech., 5, 2069–2080, doi:10.5194/amt-5-2069-2012, 2012.

Kusakabe, M. and Matsuhisa, Y.: Oxygen three-isotope ratios of silicate reference materials determined by direct comparison with VSMOW-oxygen, Geochem. J., 42, 309–317, 2008.

Landais, A., Barkan, E., and Luz, B.: Record of delta O-18 and O-17-excess in ice from Vostok Antarctica during the last 150 000 years, Geophys. Res. Lett., 35, L02709, doi:10.1029/2007GL032096 2008.

Lin, Y., Clayton, R. N., and Groening, M.: Calibration of δ^{17}O and δ^{18}O of international measurement standards – VSMOW, VSMOW2, SLAP, and SLAP2, Rapid Comm. Mass Spec., 24, 773–776, 2010.

Luz, B. and Barkan, E.: Variations of ^{17}O/^{16}O and ^{18}O/^{16}O in meteoric waters, Geochim. Cosmochim. Acta, 74, 6276–6286, 2010.

Masson-Delmotte, V., Jouzel, J., Landais, A., Stievenard, M., Johnsen, S. J., White, J. W. C., Werner, M., Sveinbjornsdottir, A., and Fuhrer, K.: GRIP deuterium excess reveals rapid and orbital-scale changes in Greenland moisture origin, Science, 309, 118–121, 2005.

Matsuhisa, Y., Goldsmith, J. R., and Clayton, R. N.: Mechanisms of hydrothermal crystallization of quartz at 250 °C and 15 kbar, Geochim. Cosmochim. Acta, 42, 173–182, 1978.

McKinney, C. R., McCreal, J. M., Epstein, S., Allen, H. A., and Urey, H. C.: Improvements in mass spectrometers for the measurement of small differences in isotope abundance ratios, Rev. Sci. Instrum., 21, 724–730, 1950.

Meijer, H. A. J. and Li, W. J.: The use of electrolysis for accurate δ^{17}O and δ^{18}O isotope measurements in water, Isotop. Environ. Health Stud., 34, 349–369, 1998.

Merlivat, L. and Jouzel, J.: Global Climatic Interpretation of the Deuterium-Oxygen 18 Relationship for Precipitation, J. Geophys. Res., 84, 5029–5033, 1979.

Miller, M. F.: Isotopic fractionation and the quantification of ^{17}O anomalies in the oxygen three-isotope system: an appraisal and geochemical significance, Geochim. Cosmochim. Acta, 66, 1881–1889, 2002.

Mook, W.: Environmental Isotopes in the Hydrological Cycle: Principles and Applications, Vol. I, IAEA, Unesco and IAEA, 2000.

Morville, J., Kassi, S., Chenevier, M., and Romanini, D.: Fast, low-noise, mode-by-mode, cavity-enhanced absorption spectroscopy by diode-laser self-locking, Appl. Phys. B, 80, 1027–1038., 2005.

Noone, D., Galewsky, J., Sharp, Z. D., Worden, J., Barnes, J., Baer, D., Bailey, A., Brown, D. P., Christensen, L., Crosson, E., Dong, F., Hurley, J. V., Johnson, L. R., Strong, M., Toohey, D., Van Pelt, A., and Wright, J. S.: Properties of air mass mixing and humidity in the subtropics from measurements of the D/H isotope ratio of water vapor at the Mauna Loa Observatory, J. Geophys. Res., 116, D22113, doi:10.1029/2011JD015773, 2011.

Petit, J. R., White, J. W. C., Young, N. W., Jouzel, J., and Korotkevich, Y. S.: Deuterium excess in recent Antarctic snow, J. Geophys. Res., 96, 5113–5122, 1991.

Risi, C., Landais, A., Bony, S., Jouzel, J., Masson-Delmotte, V., and Vimeux, F.: Understanding the ^{17}O excess glacial-interglacial variations in Vostok precipitation, J. Geophys. Res., 115, D10112, doi:10.1029/2008JD011535, 2010.

Rothman, L. S., Rinsland, C. P., Goldman, A., Massie, S. T., Edwards, D. P., Flaud, J.-M., Perrin, A., Camy-Peyret, C., Dana, V., Mandin, J.-Y., Schroeder, J., McCann, A., Gamache, R. R., Wattson, R. B., Yoshino, K., Chance, K. V., Jucks, K. W., Brown, L. R., Nemtchinov, V., and Varanasi, P.: The HITRAN spectroscopic database and HAWKS (HITRAN Atmospheric Workstation): 1996 edition, J. Quant. Spectrosc. Ra., 60, 665–710, 1996.

Sayres, D. S., Moyer, E. J., Hanisco, T. F., St Clair, J. M., Keutsch, F. N., O'Brien, A., Allen, N. T., Lapson, L., Demusz, J. N., Rivero, M., Martin, T., Greenberg, M., Tuozzolo, C., Engel, G. S., Kroll, J. H., Paul, J. B., and Anderson, J. G.: A new cavity based absorption instrument for detection of water isotopologues in the upper troposphere and lower stratosphere, Rev. Sci. Instrum., 80, 044102, doi:10.1063/1.3117349, 2009.

Schmidt, M., Maseyk, K., Lett, C., Biron, P., Richard, P., Bariac, T., and Seibt, U.: Concentration effects on laser-based δ^{18}O and δ^{2}H measurements and implications for the calibration of vapour measurements with liquid standards, Rapid Comm. Mass Spec., 24, 3553–3561, 2010.

Schoenemann, S. W., Schauer, A. J., and Steig, E. J.: Measurement of SLAP and GISP δ^{17}O and proposed VSMOW-SLAP normalization for ^{17}O$_{\mathrm{excess}}$, Rapid Commun. Mass Spec., 27, 582–590, 2013.

Schoenemann, S. W., Steig, E. J., Ding, Q., Markle, B. R., and Schauer, A. J.: Triple water-isotopologue record from WAIS Divide Antarctica: controls on glacial-interglacial changes in $^{17}O_{excess}$ of precipitation, J. Geophys. Res., 119, doi:10.1002/2014JD021770, in press, 2014.

Steig, E.J., Gkinis, V, Schauer A.J., Hoffnagle, J., Tan, S., and Schoenemann, S.: Cavity ring-down spectroscopy for the high-precision analysis of the triple oxygen isotope composition of water and water vapor, Mineral. Magazine, 77, 2257, 2013.

Tan, S. M.: Wavelength measurement method based on combination of two signals in quadrature, Patent US7420686 B2, Picarro, Inc., 2008.

Urey, H. C.: The thermodynamic poperties of isotopic substances, J. Chem. Soc., 562–581, 1947.

Van Trigt, R., Meijer, H. A. J., Sveinbjornsdottir, A. E., Johnson, S. J., and Kerstel, E. R. T.: Measuring stable isotopes of hydrogen and oxygen in ice by means of laser spectrometry: the Bølling transition in the Dye-3 (south Greenland) ice core, Ann. Glaciol., 35, 125–130, 2002.

Varghese, P. L. and Hanson, R. K.: Collisional narrowing effects on spectral lines shapes measured at high resolution, Appl. Opt., 23, 2376–2385, 1984.

Vaughn, B. H., White, J. W. C., Delmotte, M., Trolier, M., Cattani, O., and Stievenard, M.: An automated system for hydrogen isotope analysis of water, Chem. Geol., 152, 309–319, 1998.

Vimeux, F., Masson, V., Jouzel, J., Petit, J. R., Steig, E. J., Stievenard, M., Vaikmae, R., and White J. W. C.: Holocene hydrological cycle changes in the Southern Hemisphere documented in East Antarctic deuterium excess records, Clim. Dynam., 17, 503–513, 2001.

Wassenaar, L. I., Ahmad, M., Aggarwal, P., van Duren, M., Poltenstein, L., Araguas, L., and Kurttas, T.: Worldwide proficiency test for routine analysis of δ^2H and δ^{18}O in water by isotope-ratio mass spectrometry and laser absorption spectroscopy, Rapid Commun. Mass Spec., 26, 1641–1648, 2012.

Werle, P.: Accuracy and precision of laser spectrometers for trace gas sensing in the presence of optical fringes and atmospheric turbulence, Appl. Phys. B, 102, 313–329, 2011.

Wu, T., Chen, W. D., Kerstel, E., Fertein, E., Gao, X. M., Koeth, J., Rossner, K., and Bruckner, D.: Kalman filtering real-time measurements of H_2O isotopologue ratios by laser absorption spectroscopy at 2.73 µm, Opt. Lett., 35, 634–636, 2010.

York, D.: Least squares fitting of a straight line with correlated errors, Earth Planet. Sci. Lett., 5, 320–324, 1969.

Young, E. D., Galy, A., and Nagahara, H.: Kinetic and equilibrium mass-dependent isotope fractionation laws in nature and their geochemical and cosmochemical significance, Geochim. Cosmochim. Acta, 66, 1095–1104, 2002.